ISSN 2348 – 8034
Impact Factor- 3.155

GLOBAL JOURNAL OF ENGINEERING SCIENCE AND RESEARCHES

ANALYSIS OF PITTING BEHAVIOR ON THE MICROSTRUCTURAL CHARACTERIZATION AND MECHANICAL PROPERTIES OF 880 GRADE FLAT BOTTOM RAIL STEEL

Aakash Kumar*[1] and Prabhutosh Kumar [2]
*[1]Undergraduate Student, Department of Material Science and Metallurgical Engineering, MANIT Bhopal, INDIA
[2]Undergraduate Student, Department of Metallurgical Engineering, IIT Varanasi (BHU), INDIA

ABSTRACT

Railways are the backbone of public transport in India so the maintenance of the overall railway system is a crucial task. Among the various sections, the laid railway lines are the most important because any damage in rails can lead to a major accident. In this research paper the prime focus is on the 880 grade rails and the pitting caused by the environmental conditions. We have analyzed the effect of these pits on the mechanical properties and the microstructure of the rails. By visual inspection, there were serious concerns towards causing of undue stresses and rail defects due to these pitting. Defects such as pitting or chip formation in this case can hamper its durability, so in order to maintain the proper functioning regular analysis should be ensured.

For the evaluation and qualification of this rail, Indian railway standard IRST-12-2009 is followed. The specimen were subjected to mechanical tests like tensile and hardness measurement according to ASTM standards. Visual inspection and NDT were performed and there were defects observed in the rail head. Inclusion rating was also performed and it was observed that MnS inclusions were distributed along the rolling direction of the rail.

Keywords: *Rail steel, Pitting behavior, Microstructure, Inclusions, Mechanical properties, Non-destructive testing.*

I. INTRODUCTION

With the development of high-speed and heavy-load railway, much higher requirements are put forward for the comprehensive properties of steel rails [1]. Since fracture accidents of steel rail threaten the safety of railway transportations directly, more and more attention is paid to the quality of rail steel. The fatigue fracture is the main failure form of steel rail.

Despite substantial advantages in design, materials and non-destructive inspection, fatigue propagation in and failure of railway components remains an important issue for safety engineering which is also emphasized by a number of accidents over the last decades [2,3]. At the background of an increased volume of traffic, higher traffic speeds and higher axle loads, reliable damage tolerance design and effective maintenance methods have to be established. In addition to the fatigue load, rails are also subjected to other high mechanical loads and harsh environmental conditions. The main loading components are rolling contact pressure, shear and bending forces from the vehicle weight and thermal stresses due to restrained elongation of continuously welded rails and residual stresses from manufacturing

A crack generated on rail surface grows, in initial phase, at a shallow angle to the surface, then grows inward when reaching the critical crack length, and ends in fracture [4-6]. Since rail fracture can cause derailment with loss of life and property, the understanding of rail fracture mechanisms is important for reducing damages on the surface of rail. It has been known that the crack growth rate on rail surface depends upon the crack length and load type. Fracture of rail can be prevented by removing the crack before it reaches the critical length. Therefore, the crack growth rate needs to be estimated precisely according to the conditions of the track and load to develop maintenance plan against rail damages. HSLA steels when air and water cooled can be used as a replacement of normal rails because they have equivalent properties with better yield strength but the major problem is the economical aspect [7].

II. METHOD & MATERIAL

The experiments were performed after fabricating the specimen from a rail 1.5m long which was cut according to the specifications required. The rail used for this analysis is of 880 grade. The chemical composition of the various grades of rail steel according to the railway standard IRS-T-12-2009 [8] are as follows.

ISSN 2348 – 8034
Impact Factor- 3.155

Table 1: Standard chemical composition of various rail steel grades.

Grade	C	Mn	Si	S	P	Al	Mo	Cr
880	0.6-0.8	0.8-1.3	0.1-0.5	0.030	0.030	0.015	-	-
1080 Cr	0.6-0.8	0.8-1.2	0.5-1.1	0.025	0.025	0.004	0.20	0.8-1.2
1080HH	0.6-0.8	0.8-1.3	0.1-0.5	0.030	0.030	0.015	-	-

The mechanical properties according to the railway standard IRS-T-12-2009 are as follows.

Table 2: Standard mechanical properties of various rail steel grades.

Grade	UTS (MPa)	Yield Strength (MPa)	% Elongation	Running Hardness (BHN)
880	880	460	10	260
1080 Cr	1080	560	9	320-360
1080 HH	1080	460	10	340-390

This rail was manufactured using a steel which was made by basic oxygen or electric arc furnace process and casted continuously. The cross sectional area of the bloom shall not be less than ten times that of the rail section. For hardening of the head, suitable heat treatment is done to meet the requirements of the specification.

III. EXPERIMENTAL WORK

The specimen for the mechanical testing like tensile and hardness were fabricated using CNC lathe and EDM wire cutter. The specimens were prepared according to ASTM standards.

VISUAL INSPECTION AND NDT

The as received rails were of ~1.5m in length and it was observed that rail head surface was having large crater marks and seems to chipping off the surface rather than corrosion pitting.

NDT was carried out on the rail by ultrasonic flaw detector, Einstein IITFT make. An angular beam probe method was performed to assess the as received rail. The beam probes at 70° to the normal of rail surface and hence can detect flaws that can exist below the surface. Initially the surface of the rail head was cleaned with brush and oil was applied to ensure ultrasonic probe contact to reduce attenuation. The scan was performed on the center of the rail head surface as shown in the photograph. The length of the rail was scaled using chalk and measuring tape and the region where defect is identified is also marked.

CHEMICAL ANALYSIS AND HYDROGEN CONTENT

The chemical analysis of the Rail was carried out after sectioning the sample as per figure 1 for spectroscopy. Small pin samples were machined out from the head portion and tested for H_2 content by pin sample method using LECO-H2 analyser.

ISSN 2348 – 8034
Impact Factor- 3.155

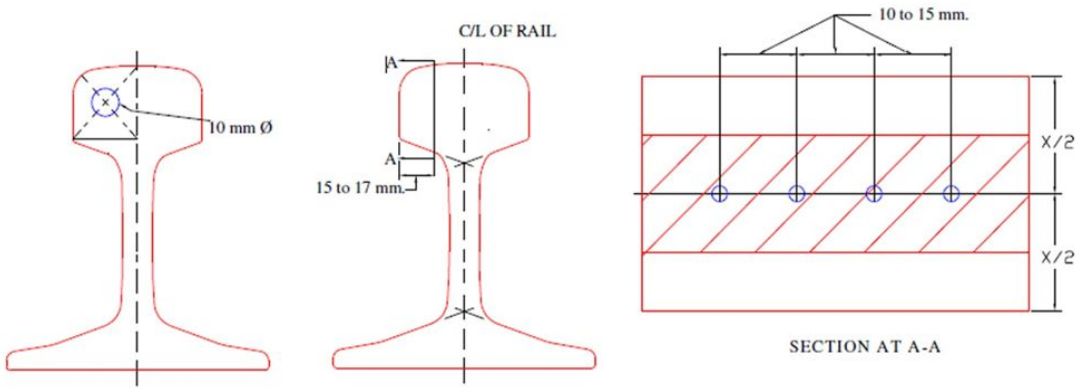

Figure 1: Location of Sample for Chemical Analysis

INCLUSION RATING

The method consists of comparing the observed field to the chart diagrams defined in this International Standard and taking in consideration separately each type of inclusion. The chart pictures correspond to square fields of view, each with an area of 0.50 mm^2, as obtained with a longitudinal plane-of-polish and as observed at 100x. Leica inclusion rating software for steel samples was used to determine the inclusion distribution in the rail along the rolling direction.

According to the shape and distribution of the inclusions, the standard diagrams are divided into five main groups, bearing the reference A, B, C, D and DS. These five groups represent the most commonly observed inclusion types and morphologies:

- Group A (sulfide type): highly malleable, individual grey particles with a wide range of aspect ratios (length/width) and generally rounded ends.
- Group B (aluminate type): numerous non deformable, angular, low aspect ratio (generally < 3), black or bluish particles (at least three) aligned in the deformation direction.
- Group C (silicate type): highly malleable, individual black or dark grey particles with a wide range of aspect ratios (generally = 3) and generally sharp ends.
- Group D (globular oxide type): non deformable, angular or circular, low aspect ratio (generally < 3), black or bluish, randomly distributed particles.
- Group DS (single globular type): circular, or nearly circular, single particle with a diameter = 13 µm.

TENSILE TESTING

Tensile specimens were prepared using IS 1608. The location of the tensile specimen can be seen in the figure 2 and the standard round tensile test piece can be seen in figure 3. The specifications of the tensile specimen used are as follows:
Diameter (D) = 10mm,
Area of cross section (A) = 78.5mm^2,
Gauge length (G) = 50mm,
Parallel length (P) = 55mm,
Radius at shoulder (R) = 10mm as shown in figure 3.

Three tensile tests were performed to procure an average value of ultimate tensile strength and yield strength.

ISSN 2348 – 8034
Impact Factor- 3.155

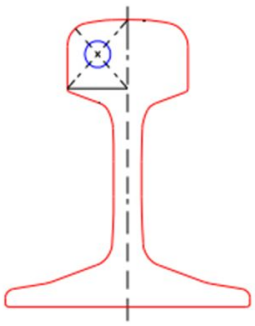

Figure 2. Location of tensile test piece

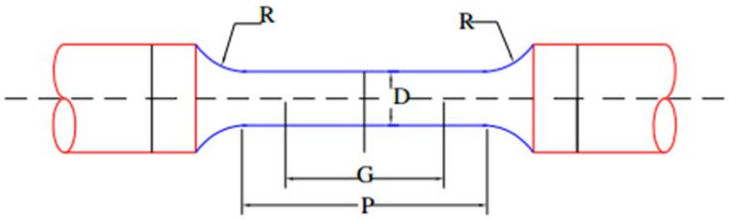

Figure 3. Standard round tensile test piece

HARDNESS, BHN

The hardness of the rail was evaluated on the rail head surface using standard Brinell hardness indentation method. For carrying out this test, impressions were made on the running tread of a test piece. This test was performed in accordance with IS: 1500. Grade 880 rail has a qualifying BHN value of 260 (minimum).

IV. RESULTS & DISCUSSIONS

VISUAL INSPECTION AND NDT

Through visual inspection there were pits all over the surface of the as received rail specimen. The size of the pits varied from very small to large ones. Fine chips were also observed which was different than pitting corrosion.

Figure 5. Sample prepared for NDT examination Rail head surfaces showing defects.

The schematic shown below indicates the position where subsurface defects are marked and shaded (color) as per severity. The analysis is qualitative and it is observed that the region where surface defects are observed, the angle probe gives subsurface defect signal which needs to be examined for after sectioning.

ISSN 2348 – 8034
Impact Factor- 3.155

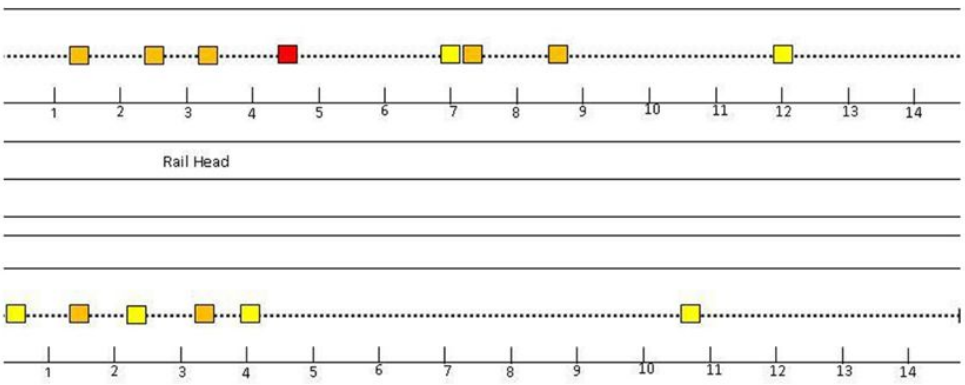

Figure 6. Schematic of defect regions identified

Ultrasonic phased array inspection was done to assess the quality of the head region esp. at location 4 of the rail BPL/SUW/2 using Omni Scan MX system with phased array (PA) module; made: Olympus. 16 elements, 5 MHz, 0.6mm pitch phased array transducer was used for this inspection and all 16 elements were used for sector scan. The inspection was carried out in the head region of the rail to detect flaws if present.

Figure 7 shows the sector image of the rail head at various positions that show the existence of the few smaller defects within the head. This was carried out to assess and confirm that the defect signal is coming from inside the rail head rather than from the surface defects.

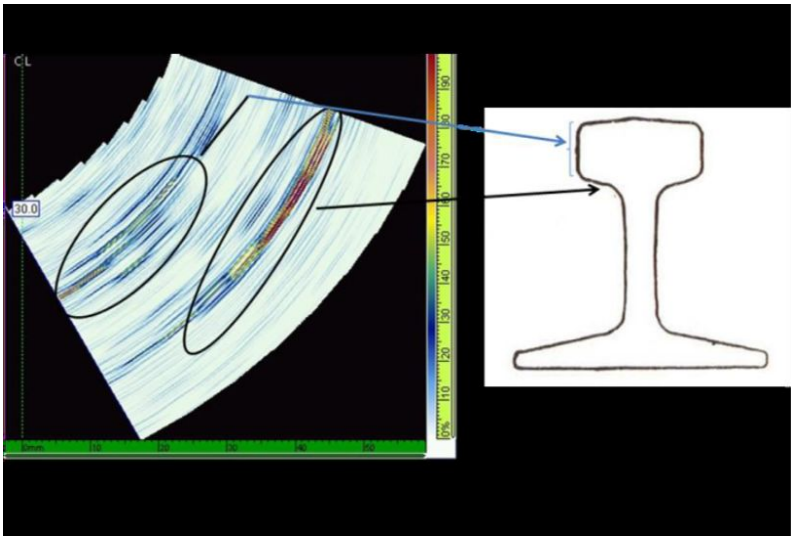

Figure 7. Schematic of defect region at location 4 identified in Phased array

CHEMICAL ANALYSIS AND HYDROGEN CONTENT

The spectrographic results indicate that the chemical composition confirms to the standard requirements of 880 grade according to table-3. But the hydrogen content exceeded the prescribed value (1.6 ppm) according to IRS-T standard.

ISSN 2348 – 8034
Impact Factor- 3.155

Table 3. Chemical analysis data of as received rail

Element	C	Si	Mn	P	S	Al	Hydrogen
Location 1	0.677	0.222	1.177	0.022	0.022	<0.001	4.1 ppm
Location 2	0.651	0.223	1.158	0.022	0.023	<0.001	4.1 ppm
Location 3	0.647	0.226	1.152	0.023	0.017	<0.001	4.1 ppm
Location 4	0.659	0.228	1.187	0.022	0.022	<0.001	4.1 ppm
Average	0.659	0.225	1.168	0.022	0.021	<0.001	4.1 ppm

From the composition analysis, the average composition of various elements are satisfying the qualifying criteria for 880 grade rail steel.

MICROSTRUCTURAL CHARACTERIZATION

The rail head was sectioned and prepared for Optical and SEM examination by standard metallographic procedure followed by etching with 2% Nital. EDS analysis was performed to understand the nature of inclusions. The as-polished samples were examined for inclusion distribution in Optical microscope. The SEM investigation showed pearlite microstructure with small ferrite grains at the pearlite boundaries. The inclusions appear to be globular and seem to be two phase with a core and periphery. The EDS examination reveals that the core of the inclusion is of MnS type and the black peripheral region is of Alumina type.

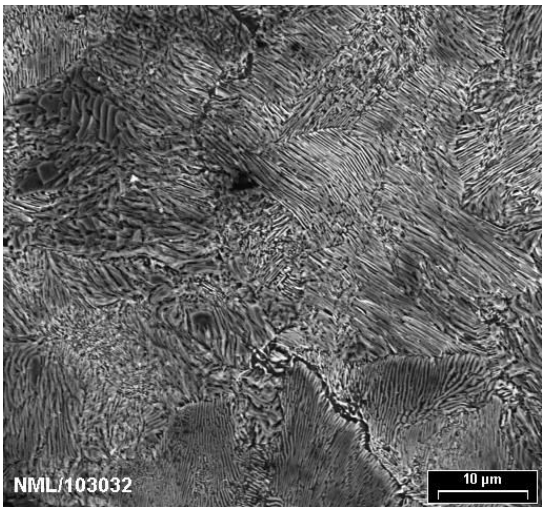

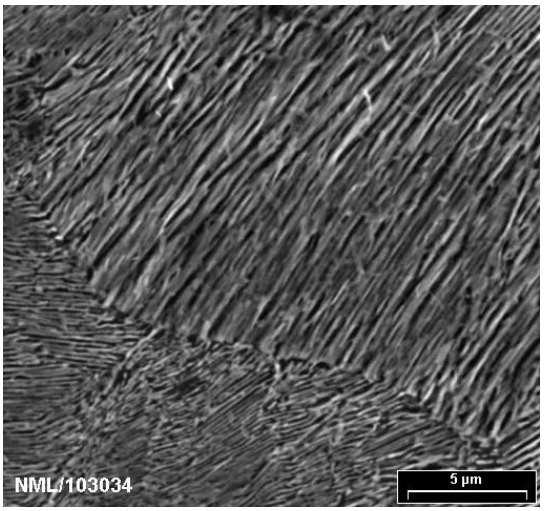

ISSN 2348 – 8034
Impact Factor- 3.155

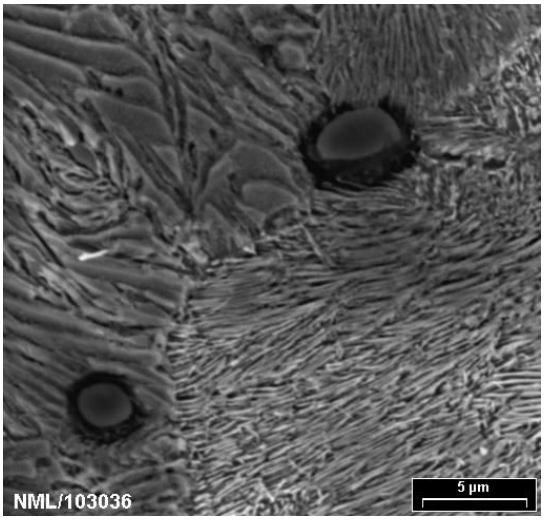

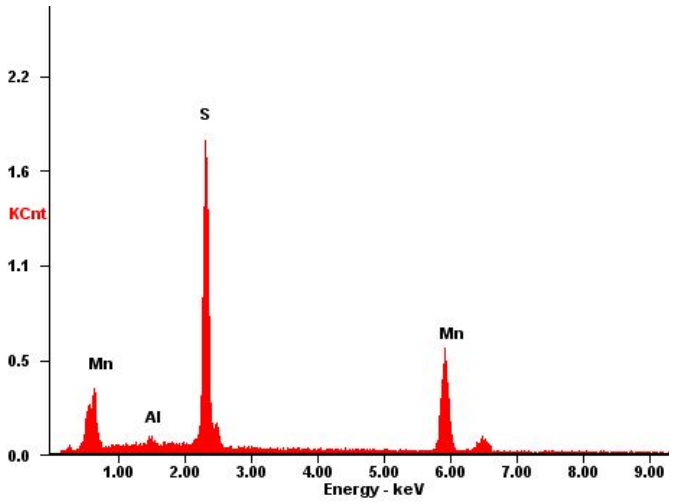

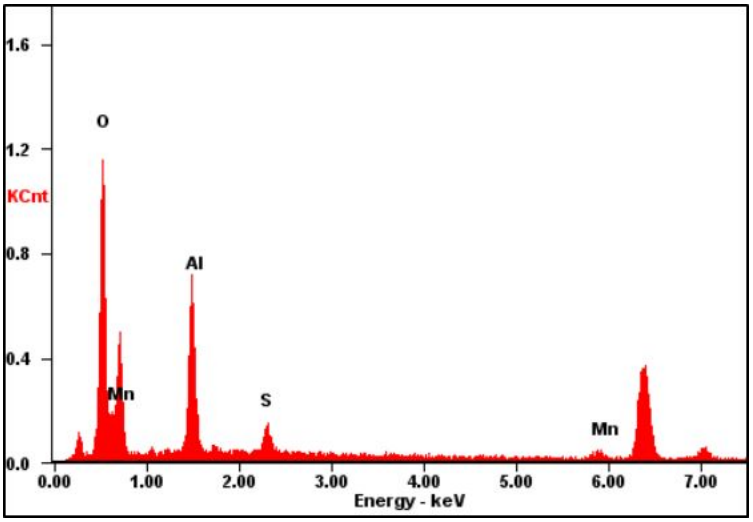

Figure 8 (a, b & c)
SEM images showing fine pearlite microstructure and globular shaped complex inclusions.
EDS analysis of inclusion from core (d) showing MnS and dark periphery (e) Showing Aluminium Oxide.

The MnS inclusion is generally observed to be elongated along the rolling direction and hence appears globular here as the sectioning plane was perpendicular to the rolling direction.

INCLUSION RATING

The inclusion distribution in the section after polishing was observed in optical microscope across the rail head. Inclusions are to be analyzed along the rolling direction of the rail. The analysis was done at 100x. Following are some of the inclusion images taken along the rolling direction and perpendicular to it. Figure 9 shows the inclusion images which are perpendicular to the rolling direction and figure 10 shows the inclusions which are along the rolling direction of the rails.

ISSN 2348 – 8034
Impact Factor- 3.155

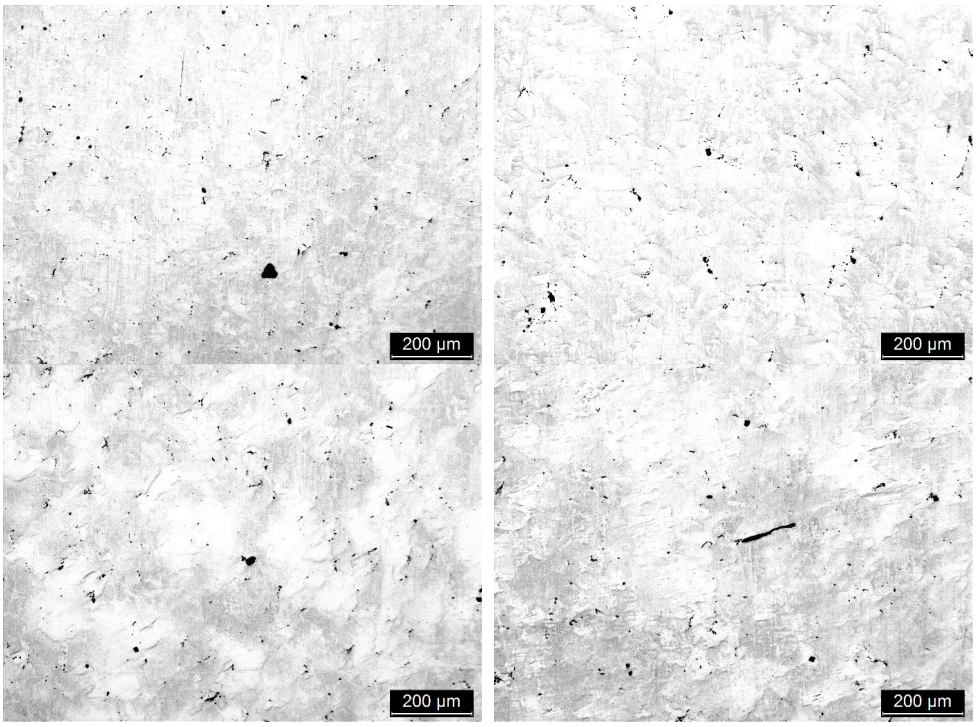

Figure 9. Inclusions along perpendicular to rolling direction

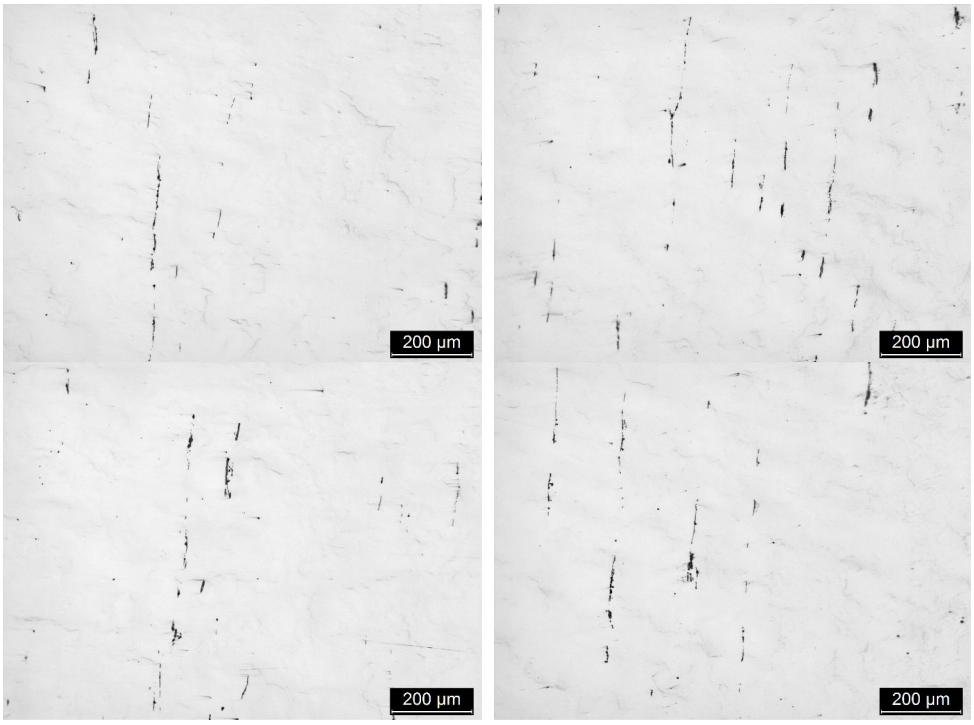

Figure 10. Inclusions along the rolling direction

ISSN 2348 – 8034
Impact Factor- 3.155

The inclusion images were analyzed using Leica inclusion rating software and then a table was prepared according to the field and type of inclusion present. Table gives the assessment of the inclusions, for a total of 24 observed fields. All the calculations were done according to ISO 4967:1998 [9].

Table 4. Indices according to the field and type of inclusion

Field	Type of inclusion								DS
	A		B		C		D		
	fine	thick	fine	thick	fine	thick	fine	thick	
1	0.5	1	0	0	0	0	0.5	0.5	0
2	0.5	1.5	0.5	0	0	0.5	0.5	0	0
3	1	2	0	0	0	0	0	0.5	0.5
4	0	2	0	0	0	0	0	0	0
5	1	1.5	0	0	0	0	0.5	0	0.5
6	0.5	1.5	0	0	0	0	0	0	0
7	0	0.5	0	0	0	0	0	0	0.5
8	0.5	1.5	0	0	0	0	0.5	0	0
9	0	1	0	0	0	0	0	0	0
10	0	1	0	0	0	0	1	0	0
11	1.5	1	0	0	0	0	0	0	0.5
12	1	1.5	0.5	0	0	0	0.5	0	0
13	0.5	1.5	0	0	0	0	0.5	0	0
14	0.5	1	0	0	0.5	0	0.5	0	0
15	0	0.5	0	0	0.5	0	0.5	0	0.5
16	0.5	1.5	0	0	0	0	0.5	0.5	0
17	0.5	1.5	0	0	0.5	0.5	0.5	0.5	0
18	0	2.5	0	0	0	0	0.5	0	0
19	0.5	0.5	0	0	0	0	0	0	0.5
20	1	0.5	0	0	0	0	0	0	0.5
21	0	1.5	0	0	0	0	0.5	0.5	0
22	0	1	0	0	0	0	0	0	0
23	0	1	0	0	0	0	0.5	0	0.5
24	2	1	0	0	0	0	1	0	0

Table 5. Total number of fields per index according to type of inclusion

Index No. (i)	Total number of fields of index i (n_i)								DS
	A		B		C		D		
	fine	thick	fine	thick	fine	thick	fine	thick	
0.5	9	4	2	0	3	2	13	5	8
1	4	8	0	0	0	0	2	0	0
1.5	1	9	0	0	0	0	0	0	0
2	0	2	0	0	0	0	0	0	0
2.5	0	1	0	0	0	0	0	0	0
3	0	0	0	0	0	0	0	0	0

ISSN 2348 – 8034
Impact Factor- 3.155

Calculation of total index (i_{tot}) and mean index (i_{moy})

$$Total\ Index\ (i_{total}) = \sum_{i=0.5}^{3} (i * n_i)$$

$$Mean\ Index\ (i_{moy}) = \frac{Total\ Index\ (i_{total})}{Total\ number\ of\ fields\ (n)}$$

Where, i = Index number
n_i = Number of fields of index i

Table 6. Showing the total index (i_{tot}) and mean index (i_{moy})

Index	Type of inclusion								DS
	A		B		C		D		
	fine	thick	fine	thick	fine	thick	fine	thick	
i_{tot}	10	30	1	0	1.5	1	8.5	2.5	4
i_{moy}	0.41	1.25	0.041	0	0.062	0.041	0.354	0.104	0.166

TENSILE TESTING

The following are the results obtained by the tensile testing of the specimen. All together there were three tests performed in order to get the average tensile properties of the rail and to validate whether it is within the specification of the standard IRST-12-2009. The results fulfilled the specifications of the railway standard. The yield strength and elongation were better than the standard values. Figure 11 shows the stress-strain plot from the three tensile tests.

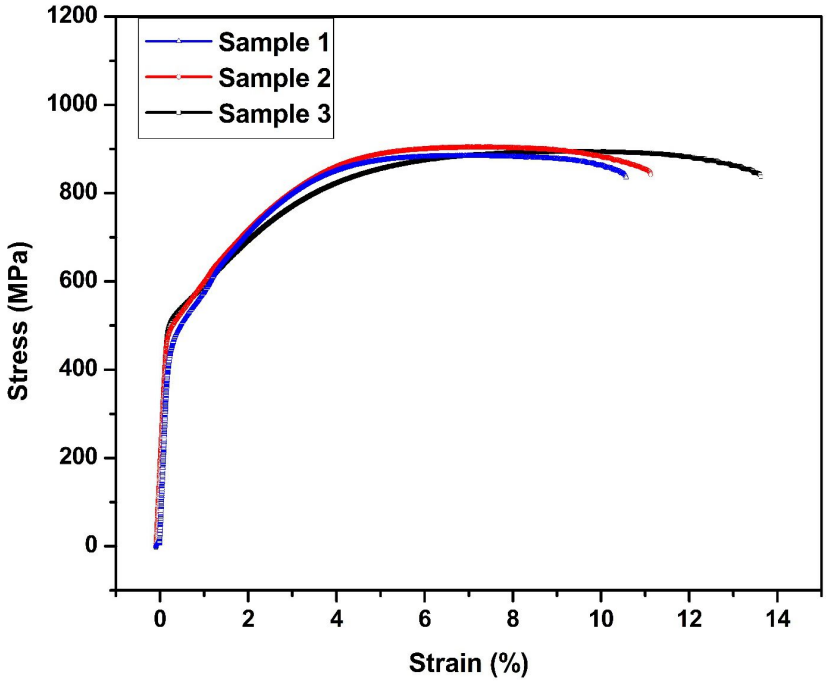

Figure 11. Showing the stress-strain plot for the three tensile rail specimen

ISSN 2348 – 8034
Impact Factor- 3.155

Table 7. Tensile data of the as received rail

Sample	Yield Strength	Ultimate tensile strength	Elongation (%)
Sample-1	525	894	13.62
Sample-2	501	905	13.98
Sample-3	507	884	13.90
Average	511	891	13.83
880 grade	460 min	880 min	10.0 min

HARDNESS, BHN

The hardness of the rail was evaluated on the rail head surface using standard Brinell hardness indentation method and results are tabulated below. It is observed that the hardness of rail head conforms to the hardness requirements of 880 rail as per the standards.

Table 8. Hardness data of as received rail

Location	1	2	3	4	5	Average
BHN	261	261	263	260	262	261

V. CONCLUSION

This paper describes the variation in the mechanical properties of rail steels due to the pitting behavior on the surface. This paper covers all the mechanical test results and the variation from the Indian railways standard were calculated. In the present investigation, the effect of pitting on the mechanical properties of the rails has been carried out and it leads to the following conclusions.

- Through visual inspection and NDT, defects were clearly visible throughout the rail surface. Ultrasonic phased array inspection confirmed the presence of small defects in the rail head.
- Chemical composition is according to the standard but hydrogen content exceeded the standard (1.6 ppm) value.
- From the microstructure characterization, pearlite microstructure with small ferrite grains at the pearlite boundaries were observed. The inclusions appear to be globular and seem to be two phase with a core and periphery. The EDS examination reveals that the core of the inclusion is of MnS type and the black peripheral region is of Alumina type.
- From the inclusion rating analysis, the amount of sulphide inclusions (MnS) was much greater than the other types of inclusions. It was observed along the rolling direction of the rails.
- The tensile properties of the analyzed rails were according to the Indian railway standard. The results exhibited better yield strength and UTS as compared to the standard values. Hardness values (BHN) was according to the standard.

ISSN 2348 – 8034
Impact Factor- 3.155

VI. ACKNOWLEDGEMENTS

The authors are very thankful to the CSIR-National Metallurgical Laboratory, Jamshedpur for their assistance in carrying out the all the required tests for this research work.

REFERENCES

1. *Li DX. Analysis of causes for rail breaking and preventative measures. Railway Stand Des 2005; 3:67–69.*
2. *Zerbst U, Beretta S. Failure and damage tolerance aspects of railway components. Eng Fail Anal 2011; 18:534-542.*
3. *Smith RA. Fatigue in transport. Problems, solutions and future threats. Trans Inst Chem E Part B 1998; 76:217–223.*
4. *Wang L, Pyzalla A, Stadlbauer W, Werner EA. Microstructure features on rolling surfaces of railway rails subjected to heavy loading, Mater Sci Eng 2003; A359:31–43.*
5. *Zhang HW, Ohsaki S, Ohnuma M, Hono K. Microstructural investigation of white etching layer on pearlite steel rail. Mater. Sci. Eng 2006; A359:191-199.*
6. *Baumann G, Fecht HJ, Liebelt S. Formation of white-etching layers on rail treads. Wear 1996; 191: 133-140.*
7. *Aakash Kumar and Ajay Dhakad., Effects of Cooling Techniques After Heat Treatment of Reinforced HSLA Steels on Their Structure, Tensile and Impact Properties. International Journal of Recent Scientific Research Vol. 6, Issue, 5, pp.4087-4090, May, 2015.*
8. *Indian Railway Standard IRST-12-2009, standard for flat bottom rails.*
9. *ISO 4967:1998. For Inclusion rating measurement.*